agronomy

MDPI

Article

Soil Organic Carbon Significantly Increases When Perennial Biomass Plantations Are Reverted Back to Annual Arable Crops

Enrico Martani [1,*], Andrea Ferrarini [1], Astley Hastings [2] and Stefano Amaducci [1]

[1] Department of Sustainable Crop Production, Università Cattolica del Sacro Cuore, Via Emilia Parmense, 84, 29122 Piacenza, Italy
[2] Institute of Biological and Environmental Sciences, School of Biological Sciences, University of Aberdeen, 23 St. Machar Drive, Aberdeen AB24 3UU, UK
* Correspondence: enrico.martani@rocketmail.com; Tel.: +39-0523-599434

Abstract: The cultivation of perennial biomass crops (PBCs) on marginal lands is necessary to provide feedstock for the bio-based EU economy and accrue environmental benefits through carbon (C) sequestration in soil. Short rotation coppice (SRC) species, e.g., willow, black locust, and poplar, and perennial rhizomatous grasses, e.g., miscanthus, switchgrass, and giant reed, have been tested in many EU projects in the last 10 years to investigate their productive potential and contribution to the mitigation of climate change. A major knowledge gap regarding PBCs is the fate of accumulated soil organic carbon (SOC), once PBC plantations are reverted to arable crops. In this study, the effects of PBCs reversion on SOC and carbon-dioxide emission (CO_2) were monitored over a 2-year period in a long-term (11-year) multispecies trial of six PBCs: Three SRC species including poplar (*Populus* spp.), willow (*Salix* spp.), and black locust (*Robinia pseudoacacia*), and three herbaceous rhizomatous grasses including miscanthus (*Miscanthus x giganteus*), switchgrass (*Panicum virgatum*), and giant reed (*Arundo donax*). The SOC change and GHG emissions were then modeled with the ECOSSE model. Two years after the reversion, SOC increased significantly for all PBCs with no significant difference between them. During the PBC cultivation phase, 5.35 Mg SOC ha^{-1} was sequestered while 10.95 Mg SOC ha^{-1} was added by reversion, which indicated that 67% of SOC sequestration occurred after the reversion. The ECOSSE model was successfully used to simulate SOC sequestration trajectories (R^2 = 0.77) and CO_2 emission from soil (R^2 = 0.82) after the reversion of the six PBCs. This indicated that the high SOC sequestration rate after the reversion was due to humification of belowground biomass (roots + rhizomes/stumps), which had been mulched and incorporated into the reversion layer (0–30 cm). This occurred in the first 2 months (on average 5.47 Mg SOC ha^{-1} y^{-1}) and in the first year after the reversion (1.3–1.8 Mg SOC ha^{-1} y^{-1}). Considering the entire PBCs cultivation cycle (13 years of PBCs + reversion), PBCs showed annual SOC sequestration rates higher than 1 Mg SOC ha^{-1} y^{-1}, placing PBCs cultivation and reversion as one of the most promising agricultural practices to combine biomass production, with the recovery of marginal lands to agricultural production through increasing the SOC.

Keywords: perennial biomass crops; soil organic carbon; ECOSSE; miscanthus; switchgrass; giant reed; black locust; poplar; willow; reversion

Citation: Martani, E.; Ferrarini, A.; Hastings, A.; Amaducci, S. Soil Organic Carbon Significantly Increases When Perennial Biomass Plantations Are Reverted Back to Annual Arable Crops. *Agronomy* **2023**, *13*, 447. https://doi.org/10.3390/agronomy13020447

Academic Editor: Di Wu

Received: 22 December 2022
Revised: 26 January 2023
Accepted: 30 January 2023
Published: 2 February 2023

1. Introduction

Perennial biomass crops (PBCs) represent a source of renewable biomass for multiple uses [1]. Historically, lignocellulosic biomass production from PBCs has been used for energetic purposes as it can be converted into second generation biofuels [2,3]. In the last years, research on PBCs has focused on the use of biomass to create high-added-value products: From biomaterials to by-products and biopolymers [1]. On the other hand, the increasing demand of biomass for energetic purposes and biobased materials to feed the growing bio-based EU economy has increased the conflicts for land use between food and

biomass [4,5]. For this reason, to reduce the above-mentioned conflicts, PBCs should be cultivated on the so-called marginal agricultural land, which are defined as land where common crops yield face technical and economical constraints in comparison with optimal conditions. Examples of marginal agricultural lands are soils with low levels of soil organic carbon (SOC), contaminated with heavy metals or abandoned soils [6]. At the European level in the last 10 years, several projects were financed to optimize the cultivation of industrial PBCs on marginal or degraded lands (Table S1). On arable lands degraded by conventional agricultural practices, PBCs can achieve consistent biomass yields [3] with few input requirements in comparison with conventional annual crops [7,8] and deliver multiple ecosystem services [9,10]. In particular, PBCs can reverse the trend of soil organic matter (SOM) decline that many intensively managed arable lands are facing. The climate benefit associated with soil C sequestration promoted by PBCs [11,12] makes their cultivation top of the list of almost all carbon farming supporting schemes in Europe [13] and around the world [14]. Attractive annual soil organic C (SOC) sequestration values in topsoil are commonly reported (0.5 Mg SOC ha^{-1} y^{-1}) as reported by [15] when annual croplands are converted to herbaceous or woody PBCs. In a recent meta-analysis, Ledo et al. [16] reported that 20-year PBCs cultivated on former arable land led to an average 20% increase in SOC at 0–30 cm (6.0 ± 4.6 Mg ha^{-1} gain). Due to their perennial nature, PBCs can also allocate consistent amounts of photoassimilated C to plant belowground organs, such as stumps and rhizomes [17]. Martani et al. [17] found that for six common PBCs, after 11 years of cultivation on a marginal soil with low SOC levels (<1%), belowground biomass C outweighs 3 times the C sequestered in soil (18.0 vs. 5.5 Mg C ha^{-1}). Annual plant C input to the soil from PBCs (litter-fall, harvest residues, and roots) combined with the absence of soil tillage, contributes to stabilizing C into soil organic matter fractions [17,18] and boosting belowground functioning [19]. Overall, the increase in SOM associated with PBCs is ultimately linked to multiple soil-based ecosystem services provision associated with their cultivation phase [5]. Nevertheless, little is known regarding the fate of belowground biomass C when PBC plantations are reconverted back to arable land and its legacy effect following annual crop rotation on the soil C sequestration trajectories. Although a large amount of literature has been produced on the potential of PBCs to sequester C during their cultivation (Ledo et al. [16] collected one hundred and eight studies available), to date only nine studies are addressing SOC changes with PBCs reversion [20]. As suggested by different authors [20,21] during reversion, belowground biomass (BGB) is incorporated into the ploughing layer. Reversion of PBCs acts as a pulse C addition to the soil of organic matter that undergoes humification and contributes to new SOM formation [15,22]. Despite the limited number of empirical studies on the reversion, several soil C models have been developed and used to estimate changes in SOC under different land-use changes [23–25], with conversion to PBCs included [7,26–29]. In particular, in the last 10 years, the Rothamsted carbon model (RothC) has been successfully used to predict SOC changes under PBCs at the laboratory [22], field [15], and regional level [30], especially on Miscanthus [29,31–33] and short rotation coppice (SRC) willow and poplar [34]. Estimation of carbon in organic soils: Sequestration and emission (ECOSSE), a process-based model developed as an evolution of RothC [35,36], has been recently tested and used successfully to simulate SOC under miscanthus [24,28] and SRC [27]. However, ECOSSE has not been used to date in order to treat and simulate the dynamics of additional pools of decomposable and resistant organic material added to the soil. It is important to study the inputs of belowground C residues at reversion [17] as well as the decay rates of these residues to depict the fate of SOC stocked after the reversion [20,22]. To encompass a better description of SOC dynamics during PBCs reversion, data from a long-term multispecies PBCs trial [17] and an incubation experiment [22] were used to calibrate and validate ECOSSE [35,36] for: (i) Modeling SOC dynamics before and after the reversion of PBCs; (ii) predicting C emission from the soil after the reversion of PBCs; (iii) quantifying C sequestration over the whole PBCs cultivation cycle, from the establishment to the reversion.

2. Materials and Methods

2.1. Experimental Field Trial

The field trial was established in April 2007 in Gariga di Podenzano, Piacenza, NW Italy (44°58048″ N, 9°41009″ E). A detailed description of the site is available in Amaducci et al. [3]. The soil is a silt loam soil classified as Haplic Luvisols (Siltic, Chromic) (FAO-WRB) with low SOC content (0.7%), carbonate content (0.41%), and neutral pH (7.2). Before planting, the site hosted a rotation of annual crops, principally maize, wheat, and tomato for 30 years (hereinafter referred to as arable land). The experimental layout was a randomized block design, with three blocks and a single plot size of 600 m^2 (20 × 30 m). Six PBCs were cultivated in the field: Three herbaceous species, giant reed (*Arundo donax* L.), switchgrass (*Panicum virgatum*), miscanthus (*Miscanthus x giganteus* L.), and three woody species, poplar (*Populus* spp.), willow (*Salix* spp.), and black locust (*Robinia pseudoacacia* spp.). A detailed description of the characteristic of the materials, plant materials, planting density, and interrow spacing is provided in Ferrarini et al. [19].

2.2. Perennial Biomass Crops Production

In addition to data published in Amaducci et al. [3], biomass production of the six PBCs in Gariga was quantified in the last three additional growing seasons before termination (2016, 2017, 2018) at complete crops senescence (winter harvest). Biomass production of herbaceous PBCs was quantified every year, by manually harvesting a known area depending on the plant density and row spacing of the crops. A biomass sub-sample was taken to the lab and then oven-dried at 105 °C to constant weight for moisture content determination. In the case of woody PBCs, biomass production was estimated with the following approach in 2018 after a 3-year cycle: (i) Stems diameter of 10 plants in a central row of the plot was measured at 1.30 m of height with a calliper; (ii) diameter values were converted to Mg ha^{-1} of dry biomass using an allometric equation specific for each woody species and provided by Facciotto et al. [37].

2.3. Reversion of the Experimental Field Trial

In March 2018, PBCs of aboveground biomass were mechanically harvested and removed from the field. PBCs were left to re-grow and then, in May 2018, glyphosate herbicide (Round-Up Platinum, Bayer Crop Science, 5 L/ha) was sprayed to stop the re-growth. The reversion of the experimental field trial was performed on 20 June 2018 due to frequent rainfalls in April and May (Figure S1). The reversion was performed to a depth of 30 cm through a forestry mulcher (Valentini, mod. Demonio, Padova, Italy and Claas Axion 980, Harsewinkel, Germany) to shred and devitalize the belowground biomass of PBCs. Immediately after the forestry mulcher, the soil was leveled and homogenized with a rotary cultivator (Carbogreen, Greenpower, Boretto, Reggio Emilia, Italy and Claas Axion 980, Harsewinkel, Germany). After reversion, the field trial hosted the following annual crop rotation: (i) Forage sorghum (sorghum x sudangrass var. sudal, June–September 2018); (ii) fallow (September 2018–May 2019); (iii) soybean (glycine max var. PR91M10, May–September 2019); and (iv) winter wheat (triticum aestivum sub. aestivum var. Taylor, October 2019–July 2020). The soil was managed with minimum tillage (MT), based on two passages of a disc-chisel to a depth of 25 cm or one passage of disk chisel at 25 cm and power harrowing at 15 cm of depth for the seedbed preparation. Irrigation was applied only after sowing (15 mm rainfall equivalent) of sorghum and soybean with a hose reel sprinkler. No fertilization was applied to the first two crops while wheat was fertilized in February 2020 with the following NP dose: 100 kg N ha^{-1} (ammonium nitrate) and 50 kg P_2O_5 ha^{-1} (monoammonium phosphate).

2.4. Soil Sampling and Carbon Analysis

A detailed description of soil sampling performed before the reversion of the site is available in Martani et al. [17]. The soil after reversion was sampled for the determination of the bulk density (BD) and C content (C_c) after each crop's harvest to a depth of 30 cm

(3, 10, 16, 24 months after reversion). SOC stock in soil was calculated in two different ways: (i) To a fixed soil depth (SOC_{DEPTH}), as the product of C_c, BD, and the width of soil layer (m) and then converted to Mg SOC ha^{-1}; and (ii) to an equivalent soil mass (SOC_{ESM}). For the equivalent soil mass (ESM) approach, a fitted cubic spline [38] was used to provide estimates of the cumulative ESM for a layer of soil mass 0–4000 Mg ha^{-1}. SOC_{ESM} was calculated by multiplying the mass of the soil by its C_c.

C_c in soil was measured on 2-mm air-dried soil samples by Dumas combustion method with an elemental analyzer VarioMax C:N (VarioMax CNS, Elementar Analysensysteme GmbH, Langenselbold, Germany). In addition, soil mini pits (0.015 m^3) were excavated to determine the amount of PBC residues immediately after the reversion and 1 year after in June 2019. Then, mini-pit material was placed in oxalic acid (2%) for 2 h, washed with a hydraulic sieving-centrifuge device [39], and oven-dried at 65 °C until constant weight. Next, the residues were sieved to quantify the proportion of residues above and below 2 mm of size.

2.5. Carbon Dioxide Emission from Soil

The CO_2 emissions from the soil after the reversion were measured using a portable infra-red gas analyzer combined with the SRC-2 soil Respiration Chamber (PP Systems, Inc., 110 Haverhill Rd, Suite 301, Amesbury, MA 01913, USA). The respiration chamber has a surface area of 78 cm^2 and a system volume of 1117 mL. The measurement time was 180 s. Two PVC collars of 25 cm in length were installed in each plot at 20 cm depth with 5 cm exceling soil surface. Collars were removed the day before soil cultivation and reinstalled the day after and left to set. To prevent leakage of CO_2 a rubber ring between the respiration chamber and the collar was used as a seal for every measurement. Respiration rates were corrected for the increase in volume of the system. High-frequency measurements (0, 1, 2, 4, 7, 9, 13, 19, 26, 33 days after reversion) were performed during the first month after the reversion and monthly over the 2 years.

2.6. Annual Crops Yield after Reversion

Total biomass, composed of dry grain yield and harvest residues, of each annual food crop was measured by manually harvesting a fixed m^2 area per plot (>2 m^2 on average). In the case of a grain crop (soybean or wheat), grain was separated from harvest residues with a Cicoria "Plot 2375" thresher machinery (Cicoria, San Gervasio, Italy). Dry weights of grain and residues for all harvested areas were measured after oven drying at 65 °C to constant weight. A sub-sample was weighed and used to determine C and N concentration by Dumas combustion method with an elemental analyzer VarioMax C:N ((VarioMax CNS, Elementar Analysensysteme GmbH, Langenselbold, Germany). The above ground residue-derived C input to the soil was calculated by multiplying the weight of the residue biomass excluding the grain by its C_c. Harvest index (HI) was calculated for every crop as the ratio between the amount of grain or biomass harvested over the total amount of biomass (grain + residues) produced by a crop.

2.7. ECOSSE Model

The ECOSSE model was developed to simulate highly organic soils, from concepts originally derived for mineral soils in the RothC model [40–42] and in the Rothamsted Nitrogen Turnover model (SUNDIAL) [43,44]. It can be used to carry out site-specific simulations with detailed input data, or national-scale simulations using the limited data typically available at larger scales. A full description of the model can be found in Smith et al. [35,36]. Similarly to RothC, the ECOSSE model uses a pool-type approach: It includes five pools of soil organic matter (SOM), namely decomposable plant material (DPM), resistant plant material (RPM), soil microbial biomass (BIO), humified organic matter (HUM), and inert organic matter (IOM). Each pool, except for IOM, follows first-order decay kinetics (DPM; k = 10 yr^{-1}, RPM; k = 0.30 yr^{-1}, BIO; k = 0.66 yr^{-1}, HUM; k = 0.02 yr^{-1}) and is considered as well mixed and chemically homogeneous. The decomposition rate is assumed to be

controlled by the available substrate. Addition or loss of C and N from different vegetation types is estimated using the C and N amounts in different parts of the plant (i.e., in the case of grain crops straw, chaff, and stubble) and harvest index. Total SOC and IOM amounts are added as inputs. Inputs from plant material are divided into resistant and decomposable material, based on a DPM/RPM ratio of 1.44 (as used in the RothC model). The site-specific ECOSSE input requirements are: Climate/atmospheric data (daily rainfall, mean daily temperature, potential evapotranspiration) (Figure S1); and nitrogen deposition rate (Table S9). The soil data inputs are: Soil pH, soil clay content, initial SOC stock, inert organic C content, soil water available at field capacity, soil water available at saturation, soil water content at wilting point, and depth to impermeable layer (Table S9). Soil water content at field capacity and wilting point was measured using Richard's apparatus. Land use/land management inputs data are: Land use for each simulation year and land use prior to simulation period, type, and yield of the current and previous crops, amount, type, and timing of fertilizer and manure application, whether or not crop residues are incorporated. The site-specific version of ECOSSE can simulate four different cultivation types, zero tillage or no-tillage (with or without mulching), minimum-tillage (5–10 cm of depth), reduced tillage (15–20 cm of depth), and conventional inversion tillage. In addition, the site-specific version of ECOSSE allows for switching between 14 different manure types and a precise description of the crops that are cultivated in the field. ECOSSE currently allows for a maximum of 36 different crops that can be parametrized [45].

2.8. Model Calibration

The site-specific version of the ECOSSE model was calibrated and run to simulate SOC dynamics and CO_2 emissions during two distinct phases: Phase (1) perennial crop cycle (from establishment until the day before reversion); and Phase (2) reversion and annual crops cycle (2-year annual crop rotation from reversion day). Some adjustments were necessary for both phases to account for the differences between crops in rotation, the amendment type (e.g., BGB incorporation at reversion), and soil cultivation systems, respectively. The initialization of the model was based on the assumption that the soil column is at a steady-state under the initial land use at the start of the simulation. Previous work has used SOC measured at a steady-state to determine the plant inputs that would be required to achieve an equivalent simulated value (e.g., Smith et al.) [35]. This approach iteratively adjusts plant inputs until measured and simulated values of SOC converge. Air temperature (°C), precipitation (mm), and potential evapotranspiration (PET, mm day^{-1}) data were measured by a nearby automated Watchdog 2000 Series (Spectrum Technologies, 3600 Thayer Court, Aurora, IL, USA) weather station (<1 km of distance).

2.8.1. Perennial Crop Cycle

The six PBCs considered in this study were parameterized in the model. To reproduce the perennial cycle of the crops we used zero-tillage cultivation, setting the date of sowing/transplant of the PBCs the day after the winter harvest, to simulate the re-growth of the PBCs in the following growing season. The annual C input to the soil from the PBCs was calculated according to Farina et al. [30] (Tables S2–S5). Yields and HI of the six perennial crops were obtained from Amaducci et al. [3] (Table S4) and from data measured as described in Section 3.1, while information about the C input from litterfall was obtained from Ferrarini et al. (unpublished). The spin-up of the model was performed using the RothC equilibrium run with the adjustment of plant input to give the measured SOC. DPM/RPM ratio was set at 1.44 for the spin-up of the model, while during perennial crop cultivation the DPM/RPM ratio was set at 0.52 for herbaceous PBCs [26] and 0.19 for woody PBCs [27].

2.8.2. Reversion and Annual Crops Cycle

After the reversion, the DPM/RPM ratio was set at 1.44 to simulate the C input from the annual crop rotation. The ECOSSE model considers two main types of C inputs to the soil: Crop residues and farmyard manure. Similar to the original version of RothC [40]

(Figure S2a), C inputs in ECOSSE are divided directly into soil DPM and RPM pools, each one characterized by a specific partitioning factor (f) and (k) decay rate. Since ECOSSE can work with multiple manure types, the parameters used to describe the different manures were modified to mimic the chemical characteristics of BGB added to the soil at reversion (Table S3). BGB of PBCs at reversion is composed of plant belowground organs (PBOs), such as stumps and rhizomes and fine roots (FR) [20]. To simulate the inputs of these two types of exogenous organic material (EOM) at reversion, PBOs and FR have been explicitly parametrized in ECOSSE as they have been shredded and incorporated into the soil.

To calibrate ECOSSE at reversion, the amount of EOM potentially incorporated into the soil of each PBC was calculated using field data ([17] as the sum of the amounts of PBO and FR biomass in the first 30 cm, the value was then scaled in accordance with the measured proportion of 2-mm sized residues, resulting from the destruction of the BGB after reversion (Table 1). To simulate the decomposition dynamic of the different EOMs added at reversion specific partitioning factors (f) and (k) decay rate values were used for ECOSSE calibration (Table 1). The original values of f and k of DPM and RPM pools in ECOSSE were: f_{DPM} = 0.49, f_{RPM} = 0.49, f_{HUM} = 0.02, k_{DPM} = 10 yr^{-1}, k_{RPM} = 0.3 yr^{-1}, and k_{HUM} = 0.02 yr^{-1}. However, with these values, the decomposition dynamics of EOM added to soil are not embedded into simulations. Crop-specific f and k values for EOM effectively incorporated at reversion at the experimental site were used. Ferrarini et al. [22], at this purpose, used a modified excel version of the RothC model [46], in which C input from EOM is split and decomposes into two additional pools: Decomposable exogenous organic matter (DEOM) and resistant exogenous organic matter (REOM) according to a specific partitioning ($f_{DEOM,\ REOM}$) and decomposition ($k_{DEOM,\ REOM}$) factor (Figure S2). The values of $f_{DEOM,\ REOM}$ and $k_{DEOM,\ REOM}$ factors used in ECOSSE in substitution of f and k values of DPM and RPM were calculated as the weighted mean between values of f and k for FR and PBO as a function of the relative contribution of FR or PBO to the total amount of EOM incorporated, and were scaled with a correction factor for real field amount of 2-mm sized residues (Table 1). The different annual crops cultivated before and after the reversion were parameterized in this study with field data and their C input to soil was calculated according to Farina et al. [30] (Tables S2 and S5) using field data (Sections 2.2–2.6). After the reversion, the DPM/RPM ratio was set at 1.44 to simulate the C input from the annual crop rotation. ECOSSE SOC simulations are based on a 50 cm depth layer. To compare simulated and measured data after the reversion (where soil samplings were performed in the 0–30 cm layer), data of the 30–50 cm layer SOC stock from Martani et al. [17] were added to data of the 0–30 cm layer SOC stock for each PBC after the reversion. This approach was selected according to the following considerations: (1) PBCs cultivation did not affect the SOC stock below 30 cm in each previous study conducted on the Gariga field [3,17,47]; (2) the reversion did not involve soil layers below 30 cm; therefore, it is not likely to have affected SOC stock in that layer.

Table 1. Amount (Mg DM ha^{-1}) of exogenous organic matter (EOM) measured by Martani et al. [17] in the reversion layer (0–30 cm depth), RothC mean partitioning (f) and decay rate (k) for EOM types (FR: Fine roots and PBO: Plant belowground organs) of six different perennial biomass crops calculated by Ferrarini et al. [22], scaled-weighted mean and 2-mm sized residues that have been used in the ECOSSE model by applying the correction factor (CF).

CROP	Plant Belowground Organs					Fine Roots					Weighted Mean					EOM Model Input	
	Amount	f_{DEOM}	f_{REOM}	k_{DEOM}	k_{REOM}	Amount	f_{DEOM}	f_{REOM}	k_{DEOM}	k_{REOM}	Amount	f_{DEOM}	f_{REOM}	k_{DEOM}	k_{REOM}	Amount	2 mm CF
	Mg DM ha^{-1}	-	-	y^{-1}	y^{-1}	Mg DM ha^{-1}	-	-	y^{-1}	y^{-1}	Mg DM ha^{-1}	-	-	y^{-1}	y^{-1}	Mg DM ha^{-1}	-
Black locust	39.40	0.39	0.61	7.9	0.39	4.27	0.10	0.90	19.5	0.21	43.67	0.36	0.64	9.0	0.37	19.64	0.45
Poplar	29.90	0.04	0.96	30.9	0.49	5.46	0.10	0.90	13.4	0.13	35.36	0.05	0.95	29.2	0.45	13.78	0.39
Willow	29.40	0.04	0.96	19.2	0.45	6.57	0.14	0.86	11.8	0.08	35.97	0.05	0.95	18.5	0.42	16.18	0.45
Miscanthus	36.00	0.08	0.92	19.6	0.47	14.33	0.12	0.88	7.3	0.02	50.33	0.09	0.91	18.4	0.42	18.61	0.37
Switchgrass	5.90	0.22	0.78	5.9	0.26	23.04	0.17	0.83	12.7	0.11	28.94	0.22	0.78	6.6	0.25	13.02	0.45
Giant reed	50.70	0.05	0.95	41.9	0.28	9.79	0.14	0.86	7.6	0.02	60.49	0.06	0.94	38.5	0.26	27.81	0.46

2.9. Carbon Sequestration Rate and Efficiency

Carbon sequestration rate (CSR) and carbon sequestration efficiency (CSE) were calculated with measured data over the whole cultivation period, from crop establishment to the reversion phase using the sampling points described in Sections 2.4 and 2.5. CSR (Mg C ha^{-1} $year^{-1}$) was calculated for a layer of soil mass of 4000 Mg ha^{-1} and over two different time periods. CSR_{PBC} was calculated to assess SOC stock changes compared with PBC establishment and CSR_{REV} to assess SOC stock changes occurring for each crop growing season after reversion. CSR_{PBC} and CSR_{REV} were calculated for each PBC as follows:

$$CSR_{PBC} = \frac{SOC_{t_i} - SOC_{t_0}}{\Delta years\left(y_{t_i} - y_{t_0}\right)}$$

$$CSR_{REV} = \frac{SOC_{t_i} - SOC_{t_{11}}}{\Delta years\left(y_{t_i} - y_{t_{11}}\right)}$$

where SOC are the measured SOC_{ESM} stock values (Mg SOC ha^{-1}), t_i is the i-th soil sampling time, t_0 is the baseline sampling time at PBCs establishment (2007), t_{11} is the sampling time before PBCs reversion (2018, 11 years after establishment), y is the year of sampling in CSR_{PBC} between t_i and t_0 and the fraction of the year in CSR_{REV} between t_i and t_{11}.

CSE (%) was calculated for each PBC over the two crop cycles (perennial cycle—CSE_{PBC} and annual crop cycle after reversion—CSE_{REV}) as follows:

$$CSE_{PBC} = \frac{SOC_{t_{11}} - SOC_{t_0}}{C\ input} \times 100$$

$$CSE_{REV} = \frac{SOC_{t_f} - SOC_{t_{11}}}{C\ input} \times 100$$

where SOC are the measured SOC_{DEPTH} stock values (Mg SOC ha^{-1}) for 0–30 cm soil layer, t_{11} is the sampling time before PBCs reversion (2018), t_f is the final sampling point 2 years after reversion (2020, after wheat harvest), C input is the amount of plant C input to soil (Mg C ha^{-1}) that enters the soil during PBCs cultivation (CSE_{PBC}) and after reversion from BGB shredding and annual crops (CSE_{REV}). C input values are those used for ECOSSE modeling (Table S5).

2.10. Statistical Analysis

SOC stocks were analyzed with a two-way mixed-model ANOVA for a complete randomized block design. Crop type (CROP factor) and sampling time (TIME factor) and their interaction (TIME × CROP) were considered as fixed main effects with block as a random effect. CSR and CSE values were analyzed with a one-way ANOVA at each sampling point. Means were compared using Tukey's honestly significant difference (alfa = 0.05). Log transformations were performed to satisfy assumptions of normality and heteroskedasticity when needed. Analyses were performed using the nlme [48] and multcomp [49] R packages. Model accuracy and performance were evaluated by calculating the root mean square error (RMSE) to measure total error, relative error (RE) to measure bias, regression coefficient (R^2) to measure the correlation between measured and modeled data and the model efficiency (ME). Analyses were performed using the HydroGOF [50] and ftsa [51] R packages.

RMSE was calculated as follows:

$$RMSE = \sqrt{\frac{\sum_{i=1}^{n}(P_i - O_i)^2}{n}}$$

where P_i is the predicted value, O_i is the observed value, and n is the sampling size.

RE was calculated as follows:

$$RE = \frac{100}{n} \sum_{i=1}^{n} \frac{(P_i - O_i)}{O_i}$$

where P_i is the simulated value, O_i is the observed value, and n is the total number of observations. The model efficiency (ME) [52] compares the squared sum of the absolute error with the squared sum of the difference between the observations and their mean value. It compares the ability of the model to reproduce the daily data variability. A negative ME value shows a poor performance, a value of zero indicates that the model does not perform better than using the mean of the observations, and values close to 1 indicate a 'near-perfect' fit [52,53], and is calculated as follows:

$$ME = 1 - \frac{\sum_{i=1}^{n}(O_i - P_i)^2}{\sum_{i=1}^{n}\left(O_i - \overline{O}\right)^2}$$

where O_i is the observed value, P_i is the simulated value, n is the total number of observations, and i is the current observation. Statistical analyses were performed using the R [54].

Graphs were produced using ggplot2 [55], ggpubr [56], and ggforce [57] R packages.

3. Results

3.1. Soil Organic Carbon Stock

Mean SOC_{DEPTH} and mean SOC_{ESM} increased significantly in the 0–30 cm soil layer 2 years after the reversion of PBCs to arable land (+24% and +30%, respectively) ($p < 0.001$, Tables S6 and S7). On average, SOC_{DEPTH} increased from a value of 37.5 Mg C ha^{-1} after 11 years of PBCs cultivation to a value of 46.6 Mg C ha^{-1} 2 years after reversion. Mean SOC_{ESM} increased from a value of 36.1 Mg C ha^{-1} after 11 years of PBCs cultivation to a value of 47.1 Mg C ha^{-1} 2 years after reversion. For both SOC_{ESM} and SOC_{DEPTH} stocks, SOC increased significantly after the reversion until fallow (May 2019, Tables S6 and S7, $p < 0.001$). No significant differences in mean SOC stock were found after soybean (September 2019) and wheat (July 2020) in comparison with fallow (Tables S6 and S7). Two years after the reversion, no significant differences were found among the SOC stock of the six PBCs for both SOC_{DEPTH} and SOC_{ESM}.

3.2. Modeling Soil CO_2 Emissions and SOC Sequestration Trajectories

The ECOSSE model was used to validate soil CO_2 (hereinafter C emission) emissions after the reversion and the dynamic of SOC from the establishment of PBCs toward the first 2 years after their reversion to annual crops cultivation. In the first 2 years after the reversion of PBCs (Figure 1), ECOSSE was able to simulate both the initial peak of C emissions that followed the incorporation of the BGB at the reversion and the dynamic of C emission for all the PBCs. The highest rates of C emission were measured in the first 3 months after the reversion when sorghum was cultivated. In this period, the C emission contributed on average to 30% of the whole C emissions of the first 2 years after the reversion of PBCs (Table 2). The average rate of C emission in the first 3 months after the reversion was 122 kg CO_2-C ha^{-1} day^{-1} (Table 2). Generally, RMSE between measured and simulated data was 54.5 kg CO_2-C ha^{-1} day^{-1} in the first 2 years after the reversion (Table 3). In the same period, the correlation between measured and modeled C emissions was high with average R^2 values of 0.82 (Table 3), RE value of −3.29%, and ME value of 0.43 (Table 3). Soil C emissions from the reversion of woody PBCs were simulated more accurately by ECOSSE than soil C emissions from herbaceous PBCs reversion (Table 3). In particular, soil C emissions from woody PBCs were under-estimated by ECOSSE (−24.4% of RE, Table 3), while C emissions from herbaceous PBCs were over-estimated (17.8% of RE, Table 3). The correlation between modeled and measured C emission was 81% for herbaceous PBCs,

while it was 83% for woody PBCs (Table 3). Among PBCs, the RMSE values ranged from 45.7 kg CO_2-C ha^{-1} day^{-1} in the case of black locust to 63.8 kg CO_2-C ha^{-1} day^{-1} in the case of giant reed (Table 3). The RE ranged from −70.3 in the case of poplar to 26.5 in the case of switchgrass (Table 3). The highest correlation between measured and modeled C emission was found for black locust (R^2 = 0.88) and switchgrass (R^2 = 0.89) (Table 3), as well as the best result for the ME (0.68 and 0.69, respectively, Table 3). ECOSSE was able to predict the increase in SOC under PBCs cultivation (Figure 2).

At the end of PBCs cultivation, the values of SOC stock predicted by ECOSSE were within the 95% CI of the measured SOC stocks (Figure 2) for all the PBCs, while 2 years after the reversion, only miscanthus and switchgrass prediction were within the 95% CI of the measured SOC stocks values (Figure 2). Generally, SOC predictions for woody crops were closer to the measured SOC values than SOC predictions for herbaceous PBCs (Figure 2). The overall RMSE of the model was 4.98 Mg SOC ha^{-1} (Table 3). The RMSE of woody crops prediction, when considering the full cycle (PBCs + reversion) was lower than the RMSE of herbaceous crops (4.0 vs. 5.7 Mg SOC ha^{-1}, respectively). The lower values of RMSE were found for miscanthus (2.2 Mg SOC ha^{-1}) and switchgrass (3.0 Mg SOC ha^{-1}), while the highest value was for giant reed (9.3 Mg SOC ha^{-1}). On average, R^2 between modeled and measured values of SOC stocks was 0.77, with RE of −3.2 and ME of −0.32 (Table 2). On average, woody crops prediction had a higher correlation between modeled and measured SOC values than herbaceous crops (0.88 vs. 0.69, Table 3) and a higher model efficiency (0.50 vs. 0.17, Table 3). The best results of ECOSSE in terms of R^2 for SOC prediction were found for poplar and switchgrass, while the best results in terms of ME were found for miscanthus (0.87) and switchgrass (0.71) (Table 3).

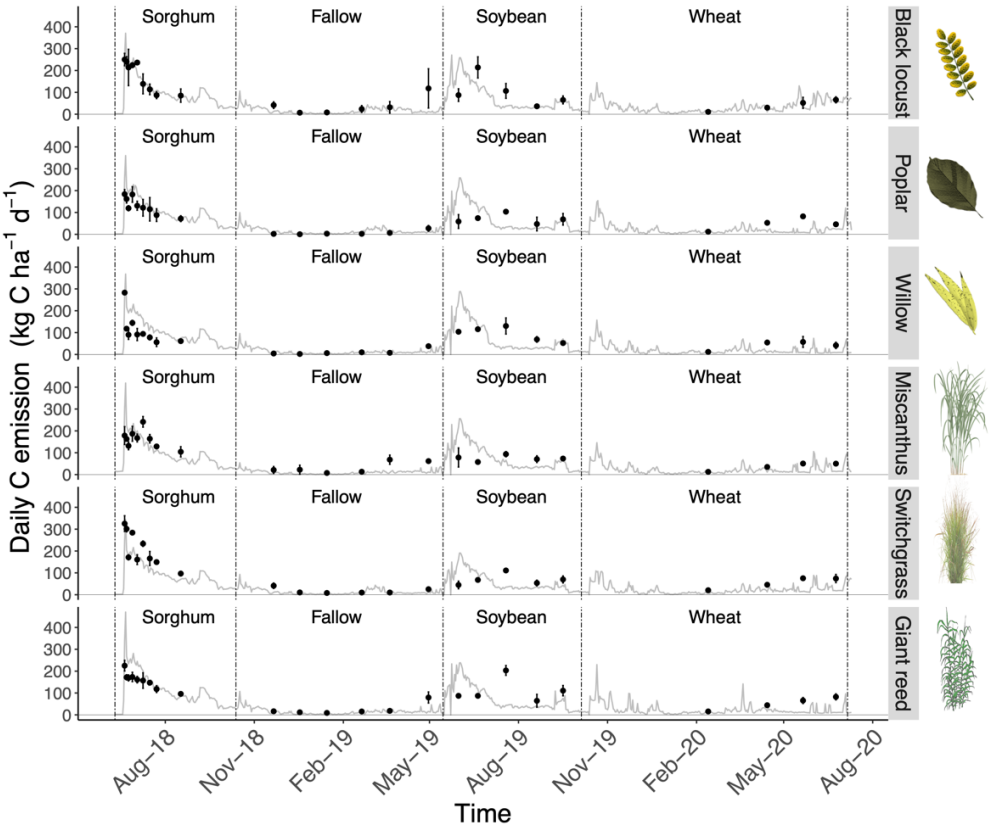

Figure 1. Results of the 2-year (2018–2020) ECOSSE simulation of C emission from soil (measured as CO_2) after the reversion of six different perennial energy crops to annual crops. The gray line represents modeled C emission, while the black dots represent measured values. Mean measured C emissions with error bars indicate 95% confidence intervals.

Table 2. Percentage over total C emission and average daily rate (kg C ha^{-1} day^{-1}) of C emission as calculated from ECOSSE simulations for each annual crop cultivated after the reversion of perennial biomass crops.

	CROP	% of Total CO_2-C Emission from Soil				Rate of CO_2 Emission (kg CO_2-C ha^{-1} day^{-1})			
		Sorghum	Fallow	Soybean	Wheat	Sorghum	Fallow	Soybean	Wheat
Average	Total	30.6	17.5	29.0	22.9	122.0	18.38	77.4	24.2
	Woody PBCs	29.5	17.8	29.3	23.4	119.6	19.1	79.3	25.4
	Herbaceous PBCs	31.6	17.2	28.8	22.4	124.4	17.7	75.5	23.0
Woody PBCs	Black locust	26.9	17.4	27.4	28.3	121.0	20.6	82.1	33.5
	Poplar	30.6	18.6	29.0	21.8	118.8	19.0	75.2	22.4
	Willow	31.0	17.5	31.4	20.1	119.1	17.6	80.4	20.4
Herbaceous PBCs	Miscanthus	30.4	15.2	31.8	22.5	119.1	15.6	82.9	23.2
	Switchgrass	31.2	18.4	26.7	23.7	111.5	17.3	63.7	22.3
	Giant reed	33.3	17.9	28.0	20.8	142.6	20.2	80.0	23.5

Table 3. Evaluation of ECOSSE performances in simulating (a) the CO_2 emission from the soil in the first 2 years within the reversion of the eleventh year of perennial biomass crop trial and (b) the soil organic carbon stock from the onset of PBCs cultivation in 2007 until the second year after the reversion (2020). Indicators are: Root mean square error (RMSE), regression coefficient (R^2), relative error (RE), and model efficiency (ME).

Parameter		CO_2-C Emission				Soil Organic Carbon (SOC)			
Level	Type	RMSE	R^2	RE	ME	RMSE	R^2	RE	ME
Model	Overall	54.52	0.82	−3.29	0.44	4.98	0.77	−3.23	0.32
	Woody PBCs	51.88	0.83	−24.37	0.42	4.05	0.88	−3.13	0.50
	Herbaceous PBCs	57.03	0.81	17.78	0.44	5.75	0.69	−3.52	0.17
Woody PBCs	Black locust	45.72	0.88	16.59	0.68	4.52	0.88	−3.82	0.41
	Poplar	50.47	0.86	−70.33	0.19	3.61	0.93	−3.46	0.54
	Willow	58.64	0.81	−19.38	0.06	3.98	0.84	−2.10	0.53
Herbaceous PBCs	Miscanthus	53.97	0.83	14.93	0.28	2.19	0.97	−1.50	0.87
	Switchgrass	52.63	0.89	26.52	0.69	2.97	0.80	2.54	0.71
	Giant reed	63.83	0.83	11.89	0.03	9.26	0.77	−11.56	−0.67

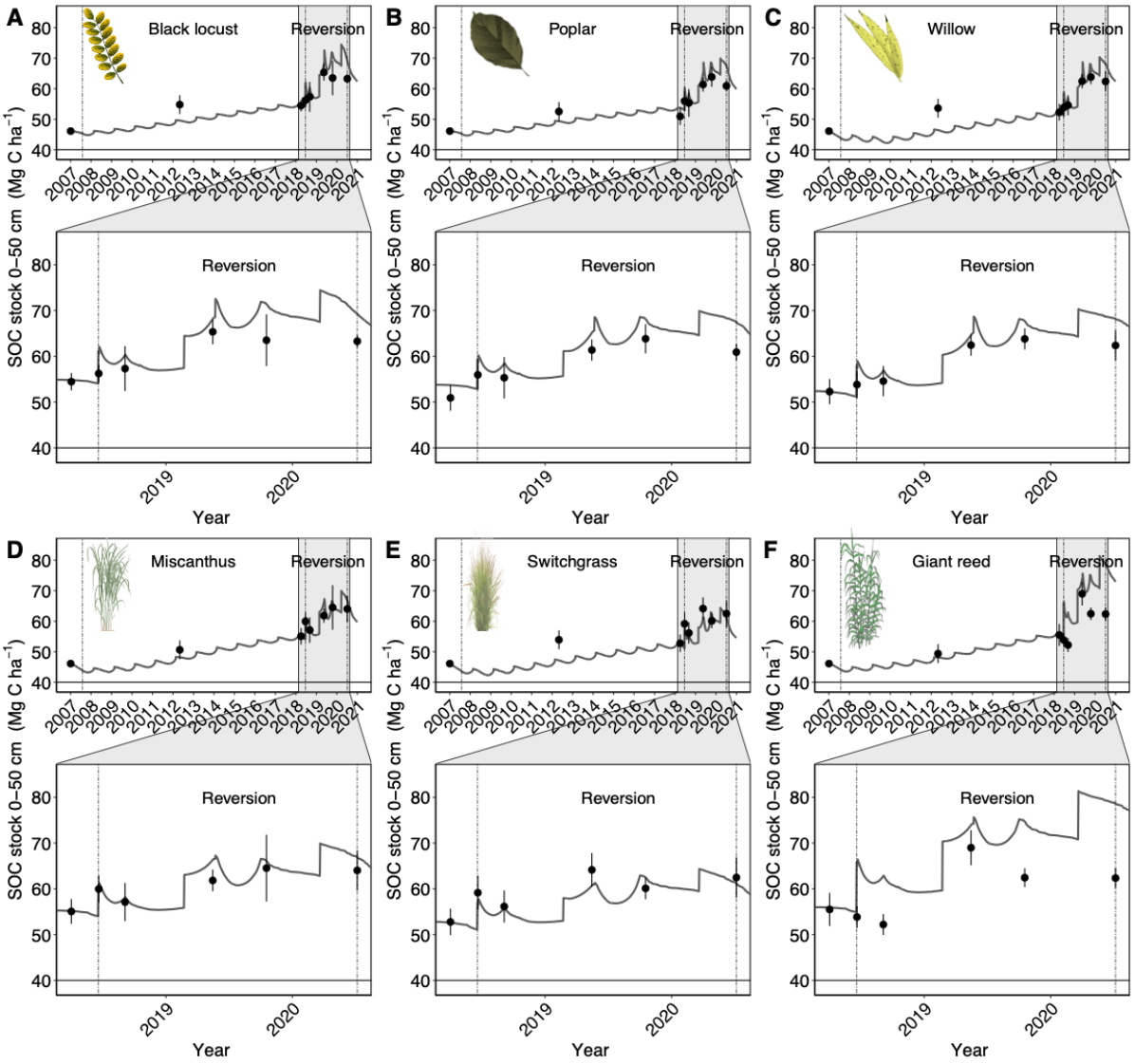

Figure 2. Results of the 13-year (2007–2020) ECOSSE simulation of soil organic carbon (SOC) under six different perennial biomass crops (2007–2018) and their reversion to annual crops (2018–2020) on a former marginal arable land. A focus on the reversion is shown for each crop: (**A**) Black locust, (**B**) poplar, (**C**) willow, (**D**) miscanthus, (**E**) switchgrass, and (**F**) giant reed. Mean SOC from soil cores obtained at different times between 2007 and 2020 are shown with error bars indicating the 95% confidence intervals.

3.3. Soil Carbon Sequestration Rate and Efficiency

CSR differed significantly among PBCs only before the reversion (p = 0.049, Table 4), with black locust having the highest CSR_{PBC} values (0.81 Mg C ha^{-1} y^{-1}, Table 4) and switchgrass the lowest (0.40 Mg C ha^{-1} y^{-1}, Table 4). After the reversion, the CSR was significantly higher (CSR_{REV} mean value: 5.5 Mg C ha^{-1} y^{-1}) than before the reversion (CSR_{PBC} mean value: 0.68 Mg C ha^{-1} y^{-1}) without significant differences among crops. Contrary to CSR_{PBC} before reversion, despite no significant differences, switchgrass had the highest CSR after the reversion (6.86 Mg C ha^{-1} y^{-1}), while black locust had the lowest (3.8 Mg C ha^{-1} y^{-1}) (Table 4). Considering the 13 years of perennial crops cultivation plus reversion, $CSR_{PBC+REV}$ was on average 1.4 Mg C ha^{-1} y^{-1} (Table 4) with no significant differences among perennial crops.

Table 4. Carbon sequestration rates (CSR, Mg SOC ha^{-1} y^{-1}) and carbon sequestration efficiency (CSE, %) considering the cultivation period (11 years of PBC cultivation—CSR_{PBC}), reversion phase (2 years of annual crop cycle after reversion—CSR_{REV}), and whole cultivation period ($CSR_{PBC+REV}$). Different letters within the same column indicate significant differences ($p < 0.05$) among crops, according to Tukey's test.

CROP		CSR (Mg SOC ha^{-1} y^{-1})			CSE (%)		
		CSR_{PBC}	CSR_{REV}	$CSR_{PBC+REV}$	CSE_{PBC}	CSE_{REV}	$CSE_{PBC+REV}$
Woody PBCs	Black locust	0.81 b	3.76	1.26	29 ab	25	27 ab
	Poplar	0.56 ab	5.07	1.25	45 abc	36	38 bc
	Willow	0.78 ab	5.86	1.56	78 b	36	50 c
Herbaceous PBCs	Miscanthus	0.64 ab	4.96	1.30	42 abc	30	33 bc
	Switchgrass	0.40 a	6.86	1.39	5 a	45	15 a
	Giant reed	0.65 ab	6.36	1.52	57 bc	18	28 ab
ANOVA	Factor	F *P*	F *P*	F *P*	F *P*	F *P*	F *P*
	CROP	3.30 0.049	1.06 0.44	1.06 0.43	6.19 0.007	2.5 0.09	14.7 0.001

CSE on average for all PBCs was 43%, 31%, and 32%, respectively for perennial crop cycle (CSE_{PBC}), annual crop cycle after reversion (CSE_{REV}), and whole cultivation period ($CSE_{PBC+REV}$). CSE differed significantly among crops both for CSE_{PBC} ($p < 0.01$, Table 4) and $CSE_{PBC+REV}$ ($p < 0.001$, Table 4). In both crop cycles, willow had the highest CSE values among PBCs (CSE_{PBC}: 78%, $CSE_{PBC+REV}$: 50%), while switchgrass had the lowest (CSE_{PBC}: 5%, $CSE_{PBC+REV}$: 15%). On the contrary, despite any significant difference compared with other PBCs, during the reversion phase, switchgrass had the highest CSE_{REV} (40%). Considering the whole PBCs cycle, from establishment to reversion, poplar, black locust, and giant reed had significantly higher CSE than switchgrass (Table 4). On average, woody PBCs had higher CSE (30%) than herbaceous PBCs (20%) considering the whole cycle.

4. Discussion

4.1. Soil Organic Carbon Sequestration Trajectories during Reversion

In the light of concerns over the impact of PBCs reversion on SOC [17,22,47], this study showed that SOC increased within the first 2 years from the reversion of PBCs: The hypothesis of an immediate loss of SOC is rejected. During PBCs cultivation, SOC is mainly accumulated in the topsoil layer (0–10 cm), as shown also by previous studies carried out in the same field at the sixth [47] and eleventh [17] year after establishment. The reversion process affected SOC stock in two different ways: (1) By distributing SOC accumulated during PBC cultivation in the top soil layer along the entire reversion soil layer (in our case 30 cm); and (2) by increasing soil respiration per unit of C added as belowground biomass. During our PBCs reversion, a soil layer was mixed and homogenized by forestry mulcher, and PBC belowground biomass (BGB) was shredded and incorporated into the soil. This pulse C input sustained SOC formation and overweighed SOC losses from the soil during the first year after the reversion (Figures 1 and 2, Table S6) [22], while between the first and second year after the reversion SOC remained stable (Figures 2 and 3). The constant C input of plant and harvest residues from the annual crop rotation under a minimum tillage regime is likely to have contributed to the stable maintenance of the new SOC level, which was formed during the first year of cultivation after reversion. These results are in agreement with previously published papers on the effect of PBCs reversion on SOC and summarized by a recent meta-analysis [20], where authors found a significant increase in SOC in the first year after the reversion of PBCs, while between the second and fifth year after the reversion, there were no significant changes in SOC stock in the reversion layer.

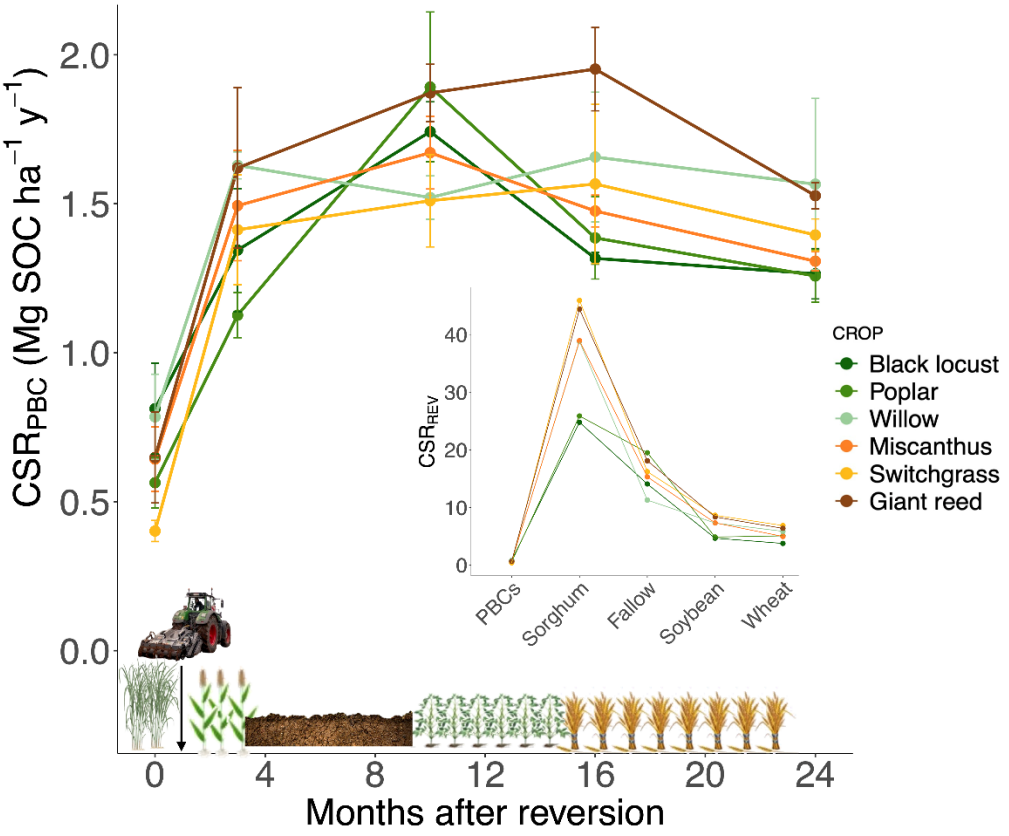

Figure 3. Carbon sequestration rates (CSR_{PBC}, Mg SOC ha^{-1} y^{-1}) and its variation (CSR_{REV}, Mg SOC ha^{-1} y^{-1}) before and after the reversion of perennial biomass crops.

Therefore, soil tillage after the reversion plays a crucial role in drawing positive soil C sequestration trajectories [20] since the positive effects of the high C pulse input at the reversion may end within the first year (Figure 3). Utilizing the RothC model, Wang et al. [58] calculated 2 Mg C ha^{-1} y^{-1} as the critical C input to maintain SOC stocks in the global wheat cropping system, while the critical C input in the European croplands is 3.1 ± 1.8 Mg C ha^{-1} y^{-1}, which is similar to the C input from annual crop rotation measured in Gariga after the reversion (3.5 Mg C ha^{-1} y^{-1}). Reversion from PBCs [59] is expected to affect soil C fluxes due to the addition of C from BGB residues [60]. Moreover, a "hotspot" period of C emissions at times of intense soil disturbance was expected to be observed during the reversion phase, as previously found by Ferrarini et al. [22] in a lab-incubation experiment that aimed to mimic the incorporation of PBCs belowground biomass. Indeed, from our field results, the incorporation of belowground biomass of PBCs at the reversion caused a peak C emission from the soil in the first days after the reversion, with a progressive reduction in the emissions already after 2 months (Figure 1). A similar initial peak of emission was found by Moore et al. [60] after the reversion of an 8-year-old switchgrass plantation to maize and by McCalmont et al. [59] after the reversion of miscanthus and SRC willow to ryegrass. These results confirm that after reversion, the pulse addition of BGB residues promotes a priming effect on previously stored SOC during the PBC cultivation cycle.

To sequester new SOC after reversion, we need to benefit from the decay of newly added organic matter from BGB residues. As argued by Janzen [61], the soil C dilemma herein is solved through a trade-off that occurred between accrual and decay during the first year after the reversion of PBCs to arable land. An intense but short period of decay occurred during the first month after reversion. During this period, the C emission contributed on average to 30% of the whole C emissions of the first 2 years after the reversion of PBCs. However, considering the first year after reversion, the building phase

of SOC prevails over the decaying one, with a significant SOC sequestration trajectory taking place (>5 Mg SOC ha^{-1} y^{-1}) supported by a good C sequestration efficiency of the BGB residues added (31% on average).

4.2. Modeling C Fluxes during Reversion of Perennial Biomass Crop to Arable Land

The ECOSSE model was originally developed to simulate C sequestration and emissions from highly-organic soils [35,36], and then calibrated to predict SOC changes under PBCs, such as miscanthus and willow [24,27,28]. In this study, in a southern European environment, the model was used to predict changes in SOC under six PBCs from the establishment toward their reversion back to arable land. The ECOSSE model well predicted SOC stock changes both under PBCs and during the reversion phase (Table 3). Adjustments were necessary to model the reversion phase for an accurate prediction of SOC dynamic (i.e., changes in f and k parameters and characteristics of the EOM input in the model). Future modifications of the SOC sub-model structure might be necessary to improve model results in simulating EOM decomposition and long-term SOC dynamics after PBCs reversion. For example, a modification of the ECOSSE model structure might be based on the modified RothC excel version tested at lab scale for BGB residues by Ferrarini et al. [20] This might improve the long-term SOC simulation of PBCs reversion as this RothC modified version accounts explicitly for differences in the quality and decomposition rates of added EOM (i.e., compost, digestates, and other crop residues, such as straw or stover). In addition to SOC prediction, the second objective of this study was to calibrate ECOSSE to simulate the C emission from the soil after the reversion. ECOSSE accurately predicted C emissions from the reversion of six PBCs with R^2 values ranging from 0.81 to 0.89 (Figure 1 and Table 3). In previous studies, ECOSSE was calibrated to simulate C and N emissions of different land uses, such as peatland [62], cropland [63], and bioenergy [64,65], while this is the first study that models daily C fluxes from the soil after the reversion of PBCs to arable land. Furthermore, other studies on the reversion of PBCs have focused on soil N_2O emissions [59] or used a different approach to measure gas exchange [60]. Similar trends of C emission from the soil after the reversion of perennial systems were found by Reinsh et al. [66] after ploughing a 16-year-old grassland, but the peak of emission reached lower values (150 kg C $ha^{-1}d^{-1}$) compared with the ones measured from the reversion of PBCs. This difference is probably due to the difference in machinery that performed the reversion (ploughing in the case of the 16-year-old grassland and forestry mulcher in the case of PBCs), quantity of BGB incorporated at the reversion (2.4 vs. 36 Mg DM ha^{-1} on average), and quality (decaying intact roots vs. shredded roots + rhizomes). These results are consistent with the conclusion of a recent meta-analysis [20] which highlighted the crucial role played by the quantity and quality of BGB input to soil during the reversion as a primary input for SOC accrual and stabilization. Our results during the reversion phase showed how ECOSSE tended to overestimate the C emissions from woody PBCs (poplar and willow in particular) and underestimate the C emission from herbaceous PBCs (Table 3). These differences are likely due to the fact that the possibility to explicitly simulate the decomposition of resistant and decomposable pool of added BGB residues to soil (Table 1) is still lacking in ECOSSE.

4.3. Carbon Sequestration Rate and Efficiency

CSR differed only before the reversion among different PBCs (Table 4). Woody PBCs showed higher CSR during PBCs cultivation than herbaceous PBCs despite the fact that they have lower C input from fine roots [17,18] and have a different potential of aboveground biomass production [3]. However, woody PBCs differ from the herbaceous one in the amount, quality, and frequency of the C input from annual leaf litterfall [67].

Providing new carbon farming solutions to growers operating in degraded soils from intensive agriculture are needed.

Our study provided clear evidence for a very high CSR (>5 Mg SOC ha^{-1} y^{-1}) in the 0–30 cm soil layer the first 2 years when PBCs are reverted to arable land (Table 4). During

the cultivation phase, on average after 11 years, a total of 5.35 Mg SOC ha^{-1} [15] were sequestered while 2 years after reversion 10.95 Mg SOC ha^{-1} were sequestered (this study). Considering the whole cultivation cycle of 13 years (cultivation + reversion) PBCs showed a mean CSR of 1.38 Mg SOC ha^{-1} y^{-1}. These results clearly demonstrate how the reversion phase is the moment where most of SOC is sequestered (67%). The cultivation phase is not relevant for sequestering C as SOC but is critical to accumulate C in the belowground organic matter in the form of fine roots and plant belowground organs. At the end of cultivation phase, Martani et al. [17] found that 68% of the belowground C stock was allocated in the BGB, and only 32% was in SOC.

Despite the fact that no significant differences in CSR among the species were observed during reversion, the main finding of this study is that the high C pulse input from BGB incorporation concurred significantly to sharpen SOC sequestration trajectory in the short-term to levels that are hard to reach by other carbon farming solutions for croplands (e.g., cover crops [68], temporary or managed grasslands [69,70], conservation tillage [71], residues incorporation [72], organic fertilization [73]). As shown in Figure 3, the peak of CSR was reached by all the PBCs, except for giant reed, 1 year after the reversion. In the case of giant reed, the peak was reached after summer 2019 (at soybean harvest): Giant reed had the highest amount of belowground biomass incorporated into the soil at the reversion (50 Mg ha^{-1} of rhizomes and 10 Mg ha^{-1} of fine roots, Table 1). Despite the fact that giant reed had the highest ratio of BGB residues in the soil after the reversion under 2-mm of size (46%, Table 1), the decomposition rate (k) of giant reed's rhizomes is the lowest (0.28 y^{-1} for the resistant pool) among plant belowground organs of PBCs. This likely contributed to a delay in the peak of SOC sequestration with respect to the other PBCs.

At the end of PBCs cultivation cycle, we found a higher average SOC sequestration rate for the woody PBCs compared with the herbaceous, confirming what was already found by Martani et al. [17]. After the reversion, instead, the herbaceous PBCs showed higher CSR values with respect to the ones of woody PBCs. This can be explained by a high amount of fine roots [17,18,47] that have been shred into the soil at the reversion (Table 1 and Figure 3). However, in general, woody PBCs had higher CSE than herbaceous PBCs after reversion; rather, the CSE is a useful indicator to quantify the amount of C input that is converted into SOC as influenced by crop-specific C input. Considering the 11 years of PBCs cultivation, willow resulted in the crop with the highest CSE, while switchgrass is the one with the lowest (Table 4). This suggests that CSE in perennial cropping systems is a trade-off between the amount of C input (herbaceous > woody) [17,18,47] and the quality of the input (woody > herbaceous) [74,75]. This becomes even more relevant during reversion in order to understand that the CSE fraction (f) and decomposition constant rate (k) of decomposable and resistant pool of added BGB residues (Table 1) need to be explicitly addressed. Interestingly, no differences were found in the CSE during the reversion period among PBCs. Given the above, it would be expected that the incorporation of BGB with a low C/N ratio, as in the case of black locust [17], resulted in significantly higher CSE at the reversion, but as already shown by Ferrarini et al. [22], the amounts of lignin, cellulose, and hemicellulose and their ratios are the most important variables controlling the decomposition of PBCs BGB in soil. Additionally, in this study, to correctly model the inputs of BGB at reversion, the "real" field C inputs have been considered as the fraction of organic matter below 2 mm that undergoes decomposition and not the amount of intact BGB that is before the reversion.

5. Conclusions

In this study, both SOC and C emissions from soil after the reversion of PBCs were reasonably well estimated using the ECOSSE model. The results from this modeling study show that ECOSSE is robust in investigating the impact of reversion of PBCs on SOC despite the fact that there are possibilities for further optimization of the model. In conclusion, the results of this study increase the reliability of PBCs cultivation as a robust and effective carbon farming solution to restore SOC in degraded soil. This suggests that the integration

into common crop rotation schemes of perennial biomass crops is also an option to restore soil health and contemporarily meet fertility and climate goals of arable food cropping systems. Nevertheless, future studies will have to elucidate the duration of legacy effect of PBCs on the SOC sequestration trajectory after reversion to understand when the SOC sequestration period will slow down or run out with annual cropping systems.

Supplementary Materials: The following supporting information can be downloaded at: https://www.mdpi.com/article/10.3390/agronomy13020447/s1. Table S1: List of the EU project aiming to improve perennial biomass crops cultivation on marginal lands; Table S2: C source and formulas to estimate the C input from plants (Mg C ha^{-1}) as adapted from Farina et al. [30]; Table S3: Parameters used to describe the belowground biomass of the perennial biomass crops in ECOSSE; Table S4: Annual biomass production (Mg DM ha^{-1}) of six different perennial biomass crops in the experimental trial of Gariga. Values from year 2007 to 2014 are taken from Amaducci et al. [3]. Data from 2015 to 2017 are unpublished data. Herbaceous perennial crops were harvested every year, while woody perennial crops were harvested every 2 or 3 years; Table S5: Biomass production (Mg DM ha^{-1}) and C inputs (Mg C ha^{-1}) of annual crops cultivated in the experimental trial of Gariga, after the reversion of six perennial biomass crops. Different letters within the same column indicate significant differences ($p < 0.05$) among crops, according to Tukey's test; Table S6: Soil organic carbon stock (Mg C ha^{-1}) in the first 30 cm of the soil before and after the reversion of six different perennial biomass crops in Gariga. Different letters within the same column indicate significant differences ($p < 0.05$) among crops, according to Tukey's test. Different letters in the timeline indicate differences ($p < 0.05$) between sampling time according to Tukey's test; Table S7: Soil organic carbon stock (Mg C ha^{-1}) based on an equivalent soil mass procedure (4000 Mg ha^{-1} of soil) before and after the reversion of six different perennial biomass crops in Gariga. Different letters within the same column indicate significant differences ($p < 0.05$) among crops, according to Tukey's test. Different letters in the timeline indicate differences ($p < 0.05$) between sampling time according to Tukey's test; Figure S1: Daily mean temperature (°C, black line), rainfalls (mm, blue bars) and potential evapotranspiration (Et0, mm, red line) in 2018, 2019 and 2020 in the field experiment of Gariga (Piacenza, NW Italy); Figure S2: Structure of the original (a) and modified (b) version of the Rothamsted Carbon model. The original version (a) is used in ECOSSE, while the modified version (b) used in Ferrarini et al. [22] to derive f and k of EOM pool; Table S8: Soil Bulk Density (g cm^{-3}) of the 0–30 cm soil layer from the beginning of Gariga experimental trial. Data of the time zero soil characterization (year 2007) were taken from Chimento et al., [47] and Amaducci et al., [3], while data of the 11th year of perennial biomass crops cultivation were taken from Martani et al., [17]. Bulk density after the reversion is the average of n = 36 samples (2 per plots); Table S9: Input parameters used for the calibration of the ECOSSE model. Arable was common for all the six PBCs, while e for the reversion phase, specific data for each species were used. [76–90] are mentioned in Supplementary Materials.

Author Contributions: Conceptualization, A.F. and E.M.; methodology, E.M., A.F. and A.H.; field measurements, E.M. and A.F.; data analysis, E.M. and A.F.; modeling, E.M. and A.H. who provided the model; writing—original draft preparation, E.M.; review and editing, A.F., S.A. and A.H. All authors have read and agreed to the published version of the manuscript.

Funding: This research was supported by funding from the Rural Developing Program (measure 16.01) of the Emilia Romagna region that financed the "FarmCO2Sink" EIP-AGRI operational group (grant number 5015651).

Informed Consent Statement: Not applicable.

Data Availability Statement: The data presented in this study are available in the article and supplemental material.

Acknowledgments: The authors thank Mike Martin for his support in the modification of the ECOSSE source code.

Conflicts of Interest: The authors declare no conflict of interest.

References

1. Scordia, D.; Cosentino, S.L. Perennial Energy Grasses: Resilient Crops in a Changing European Agriculture. *Agriculture* **2019**, *9*, 169. [CrossRef]
2. Agostini, A.; Serra, P.; Giuntoli, J.; Martani, E.; Ferrarini, A.; Amaducci, S. Biofuels from Perennial Energy Crops on Buffer Strips: A Win-Win Strategy. *J. Clean. Prod.* **2021**, *297*, 126703. [CrossRef]
3. Amaducci, S.; Facciotto, G.; Bergante, S.; Perego, A.; Serra, P.; Ferrarini, A.; Chimento, C. Biomass Production and Energy Balance of Herbaceous and Woody Crops on Marginal Soils in the Po Valley. *GCB Bioenergy* **2017**, *9*, 31–45. [CrossRef]
4. Dauber, J.; Brown, C.; Fernando, A.L.; Finnan, J.; Krasuska, E.; Ponitka, J.; Styles, D.; Thrän, D.; van Groenigen, K.J.; Weih, M.; et al. Bioenergy from "Surplus" Land: Environmental and Socio-Economic Implications. *BioRisk* **2012**, *50*, 5–50. [CrossRef]
5. Ferrarini, A.; Serra, P.; Almagro, M.; Trevisan, M.; Amaducci, S. Multiple Ecosystem Services Provision and Biomass Logistics Management in Bioenergy Buffers: A State-of-the-Art Review. *Renew. Sustain. Energy Rev.* **2017**, *73*, 277–290. [CrossRef]
6. Clifton-Brown, J.; Hastings, A.; Mos, M.; McCalmont, J.P.; Ashman, C.; Awty-Carroll, D.; Cerazy, J.; Chiang, Y.C.; Cosentino, S.; Cracroft-Eley, W.; et al. Progress in Upscaling Miscanthus Biomass Production for the European Bio-Economy with Seed-Based Hybrids. *GCB Bioenergy* **2017**, *9*, 6–17. [CrossRef]
7. Hastings, A.; Clifton-Brown, J.; Wattenbach, M.; Mitchell, C.P.; Smith, P. The Development of MISCANFOR, a New Miscanthus Crop Growth Model: Towards More Robust Yield Predictions under Different Climatic and Soil Conditions. *GCB Bioenergy* **2009**, *1*, 154–170. [CrossRef]
8. Lewandowski, I.; Clifton-Brown, J.; Trindade, L.M.; van der Linden, G.C.; Schwarz, K.U.; Müller-Sämann, K.; Anisimov, A.; Chen, C.L.; Dolstra, O.; Donnison, I.S.; et al. Progress on Optimizing Miscanthus Biomass Production for the European Bioeconomy: Results of the EU FP7 Project OPTIMISC. *Front. Plant Sci.* **2016**, *7*, 1620. [CrossRef]
9. Englund, O.; Börjesson, P.; Berndes, G.; Scarlat, N.; Dallemand, J.F.; Grizzetti, B.; Dimitriou, I.; Mola-Yudego, B.; Fahl, F. Beneficial Land Use Change: Strategic Expansion of New Biomass Plantations Can Reduce Environmental Impacts from EU Agriculture. *Glob. Environ. Chang.* **2020**, *60*, 101990. [CrossRef]
10. Lask, J.; Magenau, E.; Ferrarini, A.; Kiesel, A.; Wagner, M.; Lewandowski, I. Perennial Rhizomatous Grasses: Can They Really Increase Species Richness and Abundance in Arable Land?—A Meta-Analysis. *GCB Bioenergy* **2020**, *12*, 968–978. [CrossRef]
11. Paustian, K.; Larson, E.; Kent, J.; Marx, E.; Swan, A. Soil C Sequestration as a Biological Negative Emission Strategy. *Front. Clim.* **2019**, *1*, 8. [CrossRef]
12. Jones, M.B.; Zimmermann, J.; Clifton-Brown, J. Long-Term Yields and Soil Carbon Sequestration from Miscanthus: A Review. In *Perennial Biomass Crops for a Resource-Constrained World*; Springer International Publishing: Berlin/Heidelberg, Germany, 2016; pp. 43–49.
13. Freibauer, A.; Rounsevell, M.D.A.; Smith, P.; Verhagen, J. Carbon Sequestration in the Agricultural Soils of Europe. *Geoderma* **2004**, *122*, 1–23. [CrossRef]
14. Lemus, R.; Lal, R. Bioenergy Crops and Carbon Sequestration. *CRC Crit. Rev. Plant Sci.* **2005**, *24*, 1–21. [CrossRef]
15. Agostini, F.; Gregory, A.S.; Richter, G.M. Carbon Sequestration by Perennial Energy Crops: Is the Jury Still Out? *Bioenergy Res.* **2015**, *8*, 1057–1080. [CrossRef]
16. Ledo, A.; Smith, P.; Zerihun, A.; Whitaker, J.; Vicente-Vicente, J.L.; Qin, Z.; McNamara, N.P.; Zinn, Y.L.; Llorente, M.; Liebig, M.; et al. Changes in Soil Organic Carbon under Perennial Crops. *Glob. Chang. Biol.* **2020**, *26*, 4158–4168. [CrossRef] [PubMed]
17. Martani, E.; Ferrarini, A.; Serra, P.; Pilla, M.; Marcone, A.; Amaducci, S. Belowground Biomass C Outweighs Soil Organic C of Perennial Energy Crops: Insights from a Long-term Multispecies Trial. *GCB Bioenergy* **2020**, *13*, 459–472. [CrossRef]
18. Chimento, C.; Amaducci, S. Characterization of Fine Root System and Potential Contribution to Soil Organic Carbon of Six Perennial Bioenergy Crops. *Biomass Bioenergy* **2015**, *83*, 116–122. [CrossRef]
19. Ferrarini, A.; Martani, E.; Fornasier, F.; Amaducci, S. High C Input by Perennial Energy Crops Boosts Belowground Functioning and Increases Soil Organic P Content. *Agric. Ecosyst. Environ.* **2021**, *308*, 107247. [CrossRef]
20. Martani, E.; Ferrarini, A.; Amaducci, S. Reversion of Perennial Biomass Crops to Conserve C and N: A Meta-Analysis. *Agronomy* **2022**, *12*, 232. [CrossRef]
21. Toenshoff, C.; Stuelpnagel, R.; Joergensen, R.G.; Wachendorf, C. Carbon in Plant Biomass and Soils of Poplar and Willow Plantations-Implications for SOC Distribution in Different Soil Fractions after Re-Conversion to Arable Land. *Plant Soil* **2013**, *367*, 407–417. [CrossRef]
22. Ferrarini, A.; Martani, E.; Mondini, C.; Fornasier, F.; Amaducci, S. Short-Term Mineralization of Belowground Biomass of Perennial Biomass Crops after Reversion to Arable Land. *Agronomy* **2022**, *12*, 485. [CrossRef]
23. Anderson-Teixeira, K.J.; Masters, M.D.; Black, C.K.; Zeri, M.; Hussain, M.Z.; Bernacchi, C.J.; DeLucia, E.H. Altered Belowground Carbon Cycling Following Land-Use Change to Perennial Bioenergy Crops. *Ecosystems* **2013**, *16*, 508–520. [CrossRef]
24. Holder, A.J.; Clifton-Brown, J.; Rowe, R.; Robson, P.; Elias, D.; Dondini, M.; McNamara, N.P.; Donnison, I.S.; McCalmont, J.P. Measured and Modelled Effect of Land-Use Change from Temperate Grassland to Miscanthus on Soil Carbon Stocks after 12 Years. *GCB Bioenergy* **2019**, *11*, 1173–1186. [CrossRef] [PubMed]
25. Degryze, S.; Six, J.; Paustian, K.; Morris, S.J.; Paul, E.A.; Merckx, R. Soil Organic Carbon Pool Changes Following Land-Use Conversions. *Glob. Chang. Biol.* **2004**, *10*, 1120–1132. [CrossRef]

26. Dondini, M.; Hastings, A.; Saiz, G.; Jones, M.B.; Smith, P. The Potential of Miscanthus to Sequester Carbon in Soils: Comparing Field Measurements in Carlow, Ireland to Model Predictions. *GCB Bioenergy* **2009**, *1*, 413–425. [CrossRef]
27. Dondini, M.; Jones, E.O.; Richards, M.; Pogson, M.; Rowe, R.L.; Keith, A.M.; Perks, M.P.; Mcnamara, N.P.; Smith, J.U.; Smith, P. Evaluation of the ECOSSE Model for Simulating Soil Carbon under Short Rotation Forestry Energy Crops in Britain. *GCB Bioenergy* **2015**, *7*, 527–540. [CrossRef]
28. Dondini, M.; Richards, M.; Pogson, M.; Jones, E.O.; Rowe, R.L.; Keith, A.M.; McNamara, N.P.; Smith, J.U.; Smith, P. Evaluation of the ECOSSE Model for Simulating Soil Organic Carbon under Miscanthus and Short Rotation Coppice-Willow Crops in Britain. *GCB Bioenergy* **2016**, *8*, 790–804. [CrossRef]
29. Zimmermann, J.; Dondini, M.; Jones, M.B. Assessing the Impacts of the Establishment of Miscanthus on Soil Organic Carbon on Two Contrasting Land-Use Types in Ireland. *Eur. J. Soil Sci.* **2013**, *64*, 747–756. [CrossRef]
30. Farina, R.; Marchetti, A.; Francaviglia, R.; Napoli, R.; di Bene, C. Modeling Regional Soil C Stocks and CO_2 emissions under Mediterranean Cropping Systems and Soil Types. *Agric. Ecosyst. Environ.* **2017**, *238*, 128–141. [CrossRef]
31. Ferchaud, F.; Vitte, G.; Mary, B. Changes in Soil Carbon Stocks under Perennial and Annual Bioenergy Crops. *GCB Bioenergy* **2016**, *8*, 290–306. [CrossRef]
32. Poeplau, C. Estimating Root: Shoot Ratio and Soil Carbon Inputs in Temperate Grasslands with the RothC Model. *Plant Soil* **2016**, *407*, 293–305. [CrossRef]
33. Zatta, A.; Clifton-Brown, J.; Robson, P.; Hastings, A.; Monti, A. Land Use Change from C3 Grassland to C4 Miscanthus: Effects on Soil Carbon Content and Estimated Mitigation Benefit after Six Years. *GCB Bioenergy* **2014**, *6*, 360–370. [CrossRef]
34. Hillier, J.; Whittaker, C.; Dailey, G.; Aylott, M.J.; Casella, E.; Richter, G.M.; Riche, A.B.; Murphy, R.; Taylor, G.; Smith, P. Greenhouse Gas Emissions from Four Bioenergy Crops in England and Wales: Integrating Spatial Estimates of Yield and Soil Carbon Balance in Life Cycle Analyses. *GCB Bioenergy* **2009**, *1*, 267–281. [CrossRef]
35. Smith, J.; Gottschalk, P.; Bellarby, J.; Chapman, S.; Lilly, A.; Towers, W.; Bell, J.; Coleman, K.; Nayak, D.; Richards, M.; et al. Estimating Changes in Scottish Soil Carbon Stocks Using Ecosse. I. Model Description and Uncertainties. *Clim. Res.* **2010**, *45*, 179–192. [CrossRef]
36. Smith, J.; Gottschalk, P.; Bellarby, J.; Chapman, S.; Lilly, A.; Towers, W.; Bell, J.; Coleman, K.; Nayak, D.; Richards, M.; et al. Estimating Changes in Scottish Soil Carbon Stocks Using ECOSSE. II. Application. *Clim. Res.* **2010**, *45*, 193–205. [CrossRef]
37. Facciotto, G.; Bergante, S.; Rosso, L.; Minotta, G. Comparison between Two and Five Years Rotation Models in Poplar, Willow and Black Locust Short Rotation Coppices (SRC) in North West Italy. *Ann. Silvic. Res.* **2020**, *45*, 12–20. [CrossRef]
38. Wendt, J.W.; Hauser, S. An Equivalent Soil Mass Procedure for Monitoring Soil Organic Carbon in Multiple Soil Layers. *Eur. J. Soil Sci.* **2013**, *64*, 58–65. [CrossRef]
39. Monti, A.; Zatta, A. Root Distribution and Soil Moisture Retrieval in Perennial and Annual Energy Crops in Northern Italy. *Agric. Ecosyst. Environ.* **2009**, *132*, 252–259. [CrossRef]
40. Coleman, K.; Jenkinson, D.S. *RothC—A Model for the Turnover of Carbon in Soil*; Springer: Berlin/Heidelberg, Germany, 2014.
41. Jenkinson, D.S.; Rayner, J.H. The Turnover of Soil Organic Matter in Some of the Rothamsted Classical Experiments. *Soil Sci.* **1977**, *123*, 298–305. [CrossRef]
42. Jenkinson, D.S.; Hart, P.B.S.; Rayner, J.H.; Parry, L.C. Modelling the Turnover of Organic Matter in Long-Term Experiment Ai Rothamsted. *Intercool* **1987**.
43. Smith, J.U.; Bradbury, N.J.; Addiscott, T.M. SUNDIAL: A PC-Based System for Simulating Nitrogen Dynamics in Arable Land. *Agron. J.* **1996**, *88*, 38–43. [CrossRef]
44. Bradbury, N.J.; Jenkinson, D.S.J.; Whitmore, A.P.; Hart, P.B.S. Modelling the Fate of Nitrogen in Crop and Soil in the Years Following Application of 15N-Labelled Fertilizer to Winter Wheat. *J. Agric. Sci.* **1993**, *121*, 363–379. [CrossRef]
45. Smith, J.; Gottschalk, P.; Bellarby, J.; Richards, M.; Nayak, D.; Coleman, K.; Hillier, J.; Flynn, H.; Wattenbach, M.; Aitkenhead, M.; et al. Model to estimate carbon in organic soils–sequestration and emissions (ECOSSE). *Carbon* **2010**, *44*, 1–73. Available online: https://www.abdn.ac.uk/staffpages/uploads/soi450/ECOSSE%20User%20manual%20310810.pdf (accessed on 22 December 2022).
46. Mondini, C.; Cayuela, M.L.; Sinicco, T.; Fornasier, F.; Galvez, A.; Sánchez-monedero, M.A. Modification of the RothC Model to Simulate Soil C Mineralization of Exogenous Organic Matter. *Biogeosciences* **2017**, *14*, 3253–3274. [CrossRef]
47. Chimento, C.; Almagro, M.; Amaducci, S. Carbon Sequestration Potential in Perennial Bioenergy Crops: The Importance of Organic Matter Inputs and Its Physical Protection. *GCB Bioenergy* **2016**, *8*, 111–121. [CrossRef]
48. Pinheiro, J.; Bates, D.; R Core Team. nlme: Linear and Nonlinear Mixed Effects Models. R package version 3.1-161. 2022. Available online: https://CRAN.R-project.org/package=nlme (accessed on 22 December 2022).
49. Hothorn, T.; Bretz, F.; Westfall, P. Simultaneous Inference in General Parametric Models. *Biom. J.* **2008**, *50*, 346–363. [CrossRef]
50. Available online: https://github.com/hzambran/hydroGOF (accessed on 22 December 2022).
51. Hyndman, R.J.; Shang, H.L. ftsa: Functional Time Series Analysis. R package version 6.1. 2021. Available online: https://CRAN.R-project.org/package=ftsa (accessed on 22 December 2022).
52. Nash, J.E.; Sutcliffe, J.V. River Flow Forecasting through Conceptual Models Part I—A Discussion of Principles. *J. Hydrol.* **1970**, *10*, 282–290. [CrossRef]

53. Huang, S.; Yang, Y.; Wang, Y. A Critical Look at Procedures for Validating Growth and Yield Models. Modelling forest systems. In Proceedings of the Workshop on the Interface between Reality, Modelling and the Parameter Estimation Processes, Sesimbra, Portugal, 2–5 June 2002. [CrossRef]
54. R Core Team. *R: A Language and Environment for Statistical Computing*; R Fundation for Statstical Computing: Vienna, Austria, 2020.
55. Wickham, H. *ggplot2: Elegant Graphics for Data Analysis*; Springer-Verlag: New York, NY, USA, 2016; Available online: https://ggplot2.tidyverse.org (accessed on 22 December 2022)ISBN 978-3-319-24277-4.
56. Available online: ttps://CRAN.R-project.org/package=ggpubr (accessed on 22 December 2022).
57. Available online: https://CRAN.R-project.org/package=ggforce (accessed on 22 December 2022).
58. Wang, G.; Luo, Z.; Han, P.; Chen, H.; Xu, J. Critical Carbon Input to Maintain Current Soil Organic Carbon Stocks in Global Wheat Systems. *Nat. Publ. Group* **2016**, *6*, 19327. [CrossRef]
59. McCalmont, J.P.; Rowe, R.; Elias, D.; Whitaker, J.; McNamara, N.P.; Donnison, I.S. Soil Nitrous Oxide Flux Following Land-Use Reversion from Miscanthus and SRC Willow to Perennial Ryegrass. *GCB Bioenergy* **2018**, *10*, 914–929. [CrossRef]
60. Moore, C.E.; Berardi, D.M.; Blanc-Betes, E.; Dracup, E.C.; Egenriether, S.; Gomez-Casanovas, N.; Hartman, M.D.; Hudiburg, T.; Kantola, I.; Masters, M.D.; et al. The Carbon and Nitrogen Cycle Impacts of Reverting Perennial Bioenergy Switchgrass to an Annual Maize Crop Rotation. *GCB Bioenergy* **2020**, *12*, 941–954. [CrossRef]
61. Janzen, H.H. The Soil Carbon Dilemma: Shall We Hoard It or Use It? *Soil Biol. Biochem.* **2006**, *38*, 419–424. [CrossRef]
62. Abdalla, M.; Hastings, A.; Bell, M.J.; Smith, J.U.; Richards, M.; Nilsson, M.B.; Peichl, M.; Löfvenius, M.O.; Lund, M.; Helfter, C.; et al. Simulation of CO_2 and Attribution Analysis at Six European Peatland Sites Using the ECOSSE Model. *Water Air Soil Pollut.* **2014**, *225*, 1–14. [CrossRef]
63. Bell, M.J.; Jones, E.; Smith, J.; Smith, P.; Yeluripati, J.; Augustin, J.; Juszczak, R.; Olejnik, J.; Sommer, M. Simulation of Soil Nitrogen, Nitrous Oxide Emissions and Mitigation Scenarios at 3 European Cropland Sites Using the ECOSSE Model. *Nutr. Cycl. Agroecosyst.* **2012**, *92*, 161–181. [CrossRef]
64. Dondini, M.; Richards, M.I.A.; Pogson, M.; McCalmont, J.; Drewer, J.; Marshall, R.; Morrison, R.; Yamulki, S.; Harris, Z.M.; Alberti, G.; et al. Simulation of Greenhouse Gases Following Land-Use Change to Bioenergy Crops Using the ECOSSE Model: A Comparison between Site Measurements and Model Predictions. *GCB Bioenergy* **2016**, *8*, 925–940. [CrossRef]
65. Richards, M.; Pogson, M.; Dondini, M.; Jones, E.O.; Hastings, A.; Henner, D.N.; Tallis, M.J.; Casella, E.; Matthews, R.W.; Henshall, P.A.; et al. High-Resolution Spatial Modelling of Greenhouse Gas Emissions from Land-Use Change to Energy Crops in the United Kingdom. *GCB Bioenergy* **2017**, *9*, 627–644. [CrossRef]
66. Reinsch, T.; Loges, R.; Kluß, C.; Taube, F. Effect of Grassland Ploughing and Reseeding on CO_2 Emissions and Soil Carbon Stocks. *Agric. Ecosyst. Environ.* **2018**, *265*, 374–383. [CrossRef]
67. Xu, S.; Liu, L.L.; Sayer, E.J. Variability of Above-Ground Litter Inputs Alters Soil Physicochemical and Biological Processes: A Meta-Analysis of Litterfall-Manipulation Experiments. *Biogeosciences* **2013**, *10*, 7423–7433. [CrossRef]
68. Jian, J.; Du, X.; Reiter, M.S.; Stewart, R.D. A Meta-Analysis of Global Cropland Soil Carbon Changes due to Cover Cropping. *Soil Biol. Biochem.* **2020**, *143*, 107735. [CrossRef]
69. Bai, Y.; Cotrufo, M.F. Grassland Soil Carbon Sequestration: Current Understanding, Challenges, and Solutions. *Science* **2022**, *377*, 603–608. [CrossRef]
70. Begum, K.; Zornoza, R.; Farina, R.; Lemola, R.; Álvaro-Fuentes, J.; Cerasuolo, M. Modeling Soil Carbon Under Diverse Cropping Systems and Farming Management in Contrasting Climatic Regions in Europe. *Front. Environ. Sci.* **2022**, *10*, 819162. [CrossRef]
71. Haddaway, N.R.; Hedlund, K.; Jackson, L.E.; Kätterer, T.; Lugato, E.; Thomsen, I.K.; Jørgensen, H.B.; Isberg, P.E. How Does Tillage Intensity Affect Soil Organic Carbon? A Systematic Review. *Environ. Evid.* **2017**, *6*, 30. [CrossRef]
72. Haas, E.; Carozzi, M.; Massad, R.S.; Butterbach-Bahl, K.; Scheer, C. Long Term Impact of Residue Management on Soil Organic Carbon Stocks and Nitrous Oxide Emissions from European Croplands. *Sci. Total Environ.* **2022**, *836*, 154932. [CrossRef]
73. Gross, A.; Glaser, B. Meta-Analysis on How Manure Application Changes Soil Organic Carbon Storage. *Sci. Rep.* **2021**, *11*, 5516. [CrossRef]
74. Ferrarini, A.; Fornasier, F.; Serra, P.; Ferrari, F.; Trevisan, M.; Amaducci, S. Impacts of Willow and Miscanthus Bioenergy Buffers on Biogeochemical N Removal Processes along the Soil-Groundwater Continuum. *GCB Bioenergy* **2017**, *9*, 246–261. [CrossRef]
75. Kallenbach, C.M.; Wallenstein, M.D.; Schipanksi, M.E.; Stuart Grandy, A. Managing Agroecosystems for Soil Microbial Carbon Use Efficiency: Ecological Unknowns, Potential Outcomes, and a Path Forward. *Front. Microbiol.* **2019**, *10*, 1146. [CrossRef]
76. Monti, A.; Cosentino, S.L. Conclusive Results of the European Project OPTIMA: Optimization of Perennial Grasses for Biomass Production in the Mediterranean Area. *Bioenergy Res.* **2015**, 1459–1460. [CrossRef]
77. Scordia, D.; Papazoglou, E.G.; Kotoula, D.; Sanz, M.; Ciria, C.S.; Pérez, J.; Maliarenko, O.; Prysiazhniuk, O.; von Cossel, M.; Greiner, B.E.; et al. Towards Identifying Industrial Crop Types and Associated Agronomies to Improve Biomass Production from Marginal Lands in Europe. *GCB Bioenergy* **2022**. [CrossRef]
78. Reinhardt, J.; Hilgert, P.; von Cossel, M. Yield Performance of Dedicated Industrial Crops on Low-Temperature Characterized Marginal Agricultural Land in Europe—A Review. *Biofuels Bioprod. Biorefining* **2021**, 1–14. [CrossRef]
79. Quinkenstein, A.; Pape, D.; Freese, D.; Schneider, B.U.; Hüttl, R.F. Biomass, Carbon and Nitrogen Distribution in Living Woody Plant Parts of *Robinia pseudoacacia* L. Growing on Reclamation Sites in the Mining Region of Lower Lusatia (Northeast Germany). *Int. J. For. Res.* **2012**, *2012*, 1–10. [CrossRef]

80. Oliveira, N.; Rodríguez-Soalleiro, R.; Pérez-Cruzado, C.; Cañellas, I.; Sixto, H.; Ceulemans, R. Above- and below-Ground Carbon Accumulation and Biomass Allocation in Poplar Short Rotation Plantations under Mediterranean Conditions. *For. Ecol. Manag.* **2018**, *428*, 57–65. [CrossRef]
81. Berhongaray, G.; Janssens, I.A.; King, J.S.; Ceulemans, R. Fine Root Biomass and Turnover of Two Fast-Growing Poplar Genotypes in a Short-Rotation Coppice Culture. *Plant Soil* **2013**, *373*, 269–283. [CrossRef] [PubMed]
82. Cunniff, J.; Purdy, S.J.; Barraclough, T.J.P.; Castle, M.; Maddison, A.L.; Jones, L.E.; Shield, I.F.; Gregory, A.S.; Karp, A. High Yielding Biomass Genotypes of Willow (*Salix* spp.) Show Differences in below Ground Biomass Allocation. *Biomass Bioenergy* **2015**, *80*, 114–127. [CrossRef]
83. Amichev, B.Y.; Hangs, R.D.; Konecsni, S.M.; Stadnyk, C.N.; Volk, T.A.; Bélanger, N.; Vujanovic, V.; Schoenau, J.J.; Moukoumi, J.; van Rees, K.C.J. Willow Short-Rotation Production Systems in Canada and Northern United States: A Review. *Soil Sci. Soc. Am. J.* **2014**, *78*, S168–S182. [CrossRef]
84. Mann, J.J.; Barney, J.N.; Kyser, G.B.; di Tomaso, J.M. Miscanthus × Giganteus and Arundo Donax Shoot and Rhizome Tolerance of Extreme Moisture Stress. *GCB Bioenergy* **2013**, *5*, 693–700. [CrossRef]
85. Amougou, N.; Bertrand, I.; Machet, J.-M.M.; Recous, S. Quality and Decomposition in Soil of Rhizome, Root and Senescent Leaf from Miscanthus x Giganteus, as Affected by Harvest Date and N Fertilization. *Plant Soil* **2011**, *338*, 83–97. [CrossRef]
86. Sainju, U.M.; Allen, B.L.; Lenssen, A.W.; Ghimire, R.P. Root Biomass, Root/Shoot Ratio, and Soil Water Content under Perennial Grasses with Different Nitrogen Rates. *Field Crops Res.* **2017**, *210*, 183–191. [CrossRef]
87. Wang, W.F.; Zong, Y.Z.; Zhang, S.Q. Water-and Nitrogen-Use Efficiencies of Sweet Sorghum Seedlings Are Improved under Water Stress. *Int. J. Agric. Biol.* **2014**, *16*, 285–292.
88. He, J.; Jin, Y.; Du, Y.L.; Wang, T.; Turner, N.C.; Yang, R.P.; Siddique, K.H.M.; Li, F.M. Genotypic Variation in Yield, Yield Components, Root Morphology and Architecture, in Soybean in Relation to Water and Phosphorus Supply. *Front. Plant Sci.* **2017**, 8. [CrossRef]
89. Williams, J.D.; Mccoo, O.K.; Rea Rdo, C.L.; Douglas, C.L.; Albrecht, S.L.; Rickman, R.W. Root:Shoot Ratios and Belowground Biomass Distribution for Pacific Northwest Dryland Crops. *J. Soil Water Conserv.* **2013**. [CrossRef]
90. Rogora, M.; Arisci, S.; Marchetto, A. The Role of Nitrogen Deposition in the Recent Nitrate Decline in Lakes and Rivers in Northern Italy. *Sci. Total Environ.* **2012**, *417–418*, 214–223. [CrossRef]